Title of Thesis: Effects of depositional structure of sand on liquefaction resistance
（砂粒子の堆積構造が液状化抵抗に与える影響）

Name: Islam Md Rabiul
Supervisor: Hirofumi Toyota

1. Introduction

This study examines how the orientation of sand particles affects their ability to resist liquefaction, which is a crucial issue in geotechnical engineering, particularly in earthquakes prone areas. Liquefaction occurs mainly during the earthquake. Before the earthquake the soil particles are strong enough but during earthquake shaking destroys the soil skeleton structures through increasing pore water pressure. The impact of depositional structures of sand particles on their resistance to liquefaction are investigated in the study. Various depositional structures, considering loose packing, stratification, and particle orientations are investigated to understand their influence on the mechanical behavior of sandy soils. Youd et al. (1973) found that loose sands exhibit significant susceptibility to liquefaction under cyclic loading conditions. According to Seed & Idriss (1982), dense sands require higher cyclic stress to liquefy and it showing greater resistance. Sand with a medium density (Dr=40%) was used for these studies to investigate liquefaction resistance at various depositional angles (0°, 45° and 90°).

2. Experiments

2.1. Testing material and specimen preparation

A Japanese standard sand (Toyoura sand) was used in this study. The primary concept of particle orientation is that: in 0°, almost all the particles lies in horizontal direction, while particles tend to stand vertically in 90° (Fig. 1). The particle size distribution shows that Toyoura sand is a sub-angular to angular poorly graded fine quartz rich sand (Fig. 2). The physical parameters of the sand are shown in Table 1. A container with movable walls (Fig. 3) was employed to create a soil fabric at different deposition angles (0°, 45° and 90°). Air pluviation

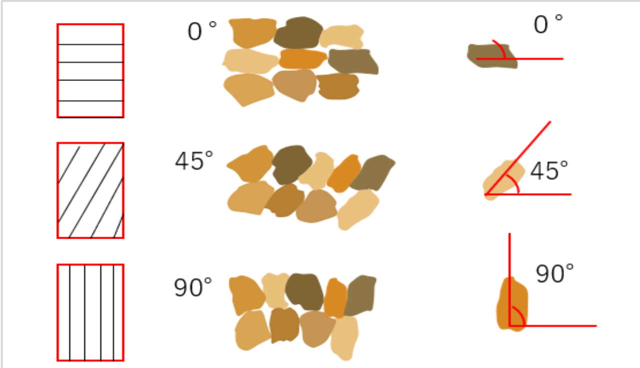

Fig. 1: Concept of particle orientation

methods has been used to make the cylindrical specimen whose diameter approximately 50 mm and height 125 mm. After the trimming procedure, the specimen is placed in the triaxial apparatus by using membrane stretcher.

Table 1: Physical parameters of Toyoura sand

SG	γd_{max} g/cm³	γd_{min} g/cm³	e_{max}	e_{min}	D50 (mm)	Cu
2.65	1.637	1.336	0.99	0.597	0.2	1.48

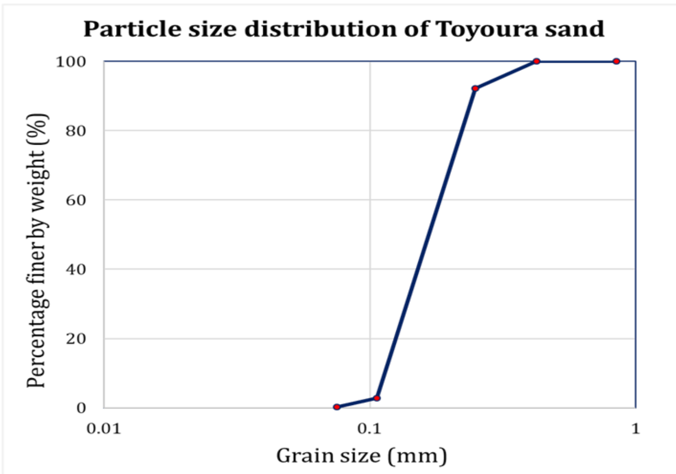

Fig. 2: Particle size distribution of Toyoura sand

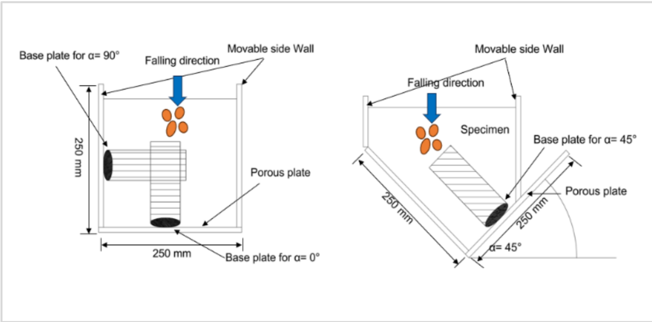

Fig. 3: Container with movable walls

The processes of making the specimen are:

- To pour the sand into the movable wall container.
- To immerse it in water for 30 minutes, then the water was dehydrated.
- Set the specimen in triaxial machine after Trimming and conducted experiment (Fig. 4).

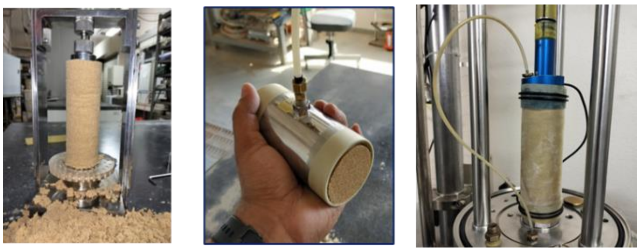

Fig. 4: Specimen trimming, membrane setup and setting into triaxial machine

2.2. Tests conducted with the triaxial apparatus

The undrain cyclic triaxial test was used for this study. Two tests, namely liquefaction strength test and bender element (BE), shown in Fig. 5 and Fig. 6, were conducted to determine the liquefaction registration of Toyoura sand considering cyclic stress ratio (CRR) and axial strain (ε_a). The characteristic of the sands is also represented by the stiffness (or initial shear modulus, G_0).

In BE test, the parameter of wave travel time (Δt) was obtained. Then the shear wave velocity (V_s) and initial shear modulus (G_0) were calculated. Shear waves are transmitted from top of the specimen by transmitter that is connected with cap. Output signals are recorded by receiver which is connected with pedestal as shown in Fig 5(a) & 5(b). Four different frequency (15, 20, 25 & 30) kHz are used and make average for (G_0) calculating.

The experiment procedure of the liquefaction test involves several steps. First, the specimen is set and then saturated through a saturation process.

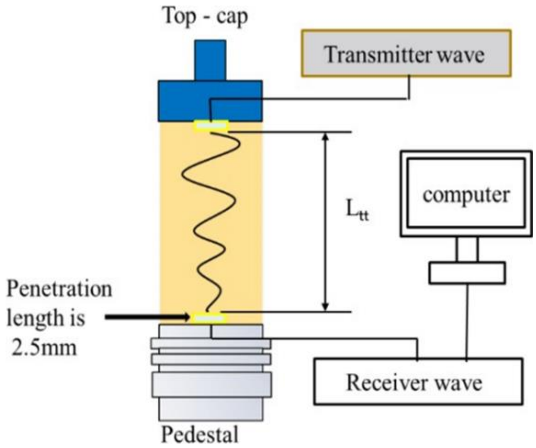

Fig. 5(a): Shear wave transfer mechanism of BE

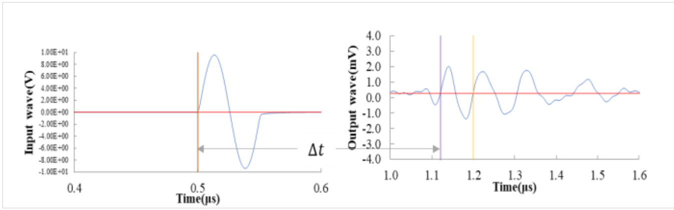

Fig. 5(b): Travel time between input and output wave

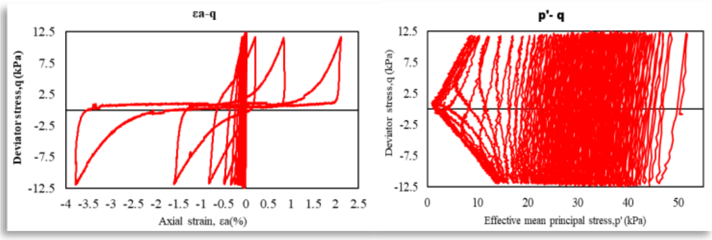

Fig. 6(a): Typical liquefaction strength curve (ε_a =1%)

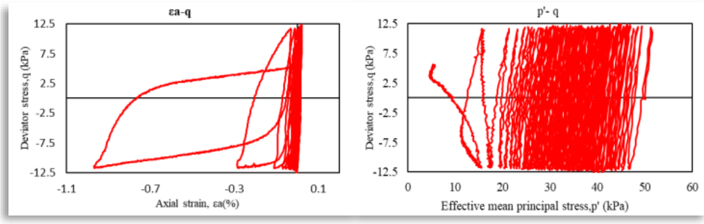

Fig. 6(b): Typical re-liquefaction strength curve (ε_a =5%)

After saturation, the specimen undergoes an initial consolidation and perform BE to determine the initial shear modulus. The specimen is then subjected to liquefaction until the axial strain reaches about 1% (about 95% of excess pore water ratio) in Fig. 6(a). After liquefaction, the specimen is re-consolidated, and BE is conducted again. The specimen undergoes re-liquefaction which stops when the axial strain reaches 5% in Fig. 6(b).

2.3. Procedure of microscopic data analysis

Throughout this process, a microscopic picture is taken before cutting the specimen and another one is taken after completing the first liquefaction in Fig. 7. The Daino Capture microscopic device is used for taking close pictures of soil particles. Before liquefaction 9 pictures are taken from observation area as shown in Fig. 7(a), as well as 9 more pictures are taken from trimmed specimen after first cyclic loading completed in Fig. 7(b).

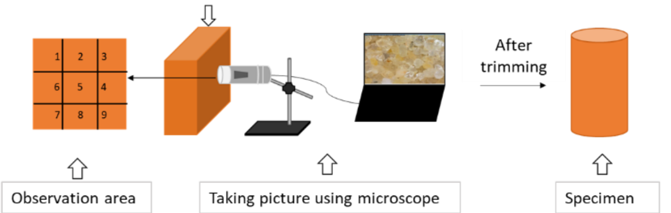

Fig. 7(a): Microscopic picture taking procedure (before liq.)

Fig. 7(b): Microscopic picture taking procedure (after liq.)

The average quantitative values of the depositional angle θ and the vector magnitude (V.M) were determined using the equation proposed by Curray (1956) to characterize the distribution of particle orientation in the prepared specimens. Equation of θ (Eqn. i) specifies that θ varies from 0° to 180°, and 'n' represents the number of observations (particles) in each group. The value of V.M (Eqn. ii) indicates the intensity of the preferred orientation of particles and ranges from zero for a completely random and unsystematic distribution of particle orientation to 100% for the same direction observed in all particles.

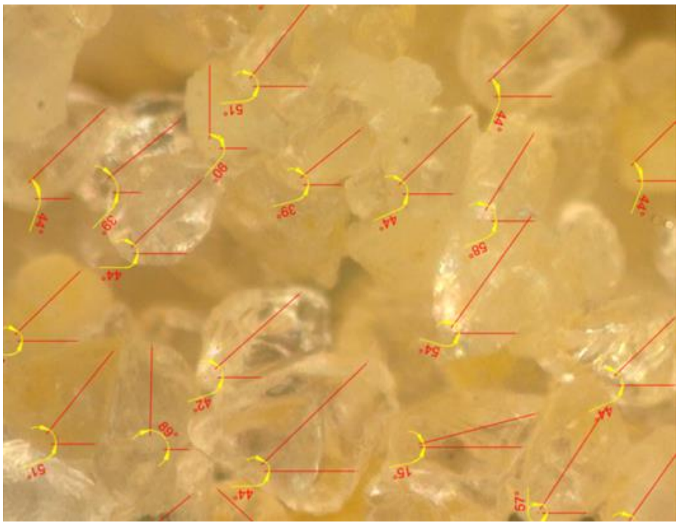

Fig. 8: Angle measurement from microscopic image

$$\theta = \frac{1}{2}\tan^{-1}\left(\frac{\sum_{i-1}^{n} sin2\theta}{\sum_{i-1}^{n} cos2\theta}\right) \text{ ----------------------------------(i)}$$

$$V.M = \frac{100}{n}\sqrt{\sum_{i-1}^{n}(Sin2\theta)^2 + (cos2\theta)^2} \text{ -------------(ii)}$$

Approximately 50 particles were measured at each position, resulting in a total of around 500 grains for each case. A typical angle measurement technique of microscopic picture is shown in Fig. 8 that is analyzed by Auto CAD 2025.

3. Results and Discussion

3.1 Bender element results

The initial shear modulus value exhibits a similar trend for relative densities of 40% and 60%. The G_0 value rises with increasing particle angle prior to liquefaction. However, because of the soil particle's contact point, the shear modulus value drops during liquefaction at 90°. The sand particles with a 90° orientation are nearly vertical in direction, indicating small number of contacting points between particles

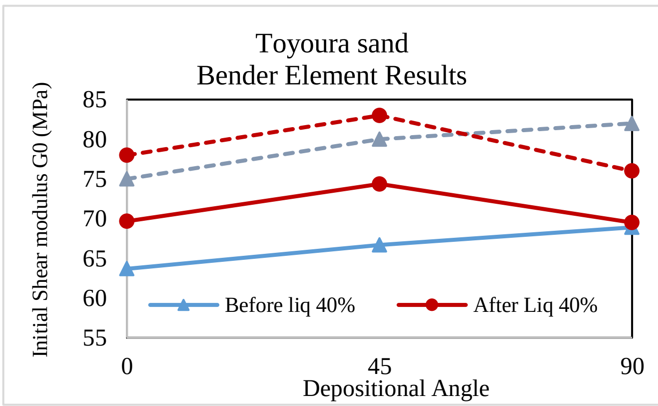

Fig. 9: Initial shear modulus before and after liquefaction

in vertical direction. The 90° shear wave velocity is higher than the others as a result. Consequently, the initial shear modulus (in Fig. 9) is greater than 0° and 45°.

3.2 Liquefaction Resistance

Fig. 10 illustrates the relationship between the cyclic stress ratio (σd/2σ') and the number of cycles to liquefaction (Nc) for Toyoura sand under undrained conditions with an effective confining stress (σ') of 50 kPa.

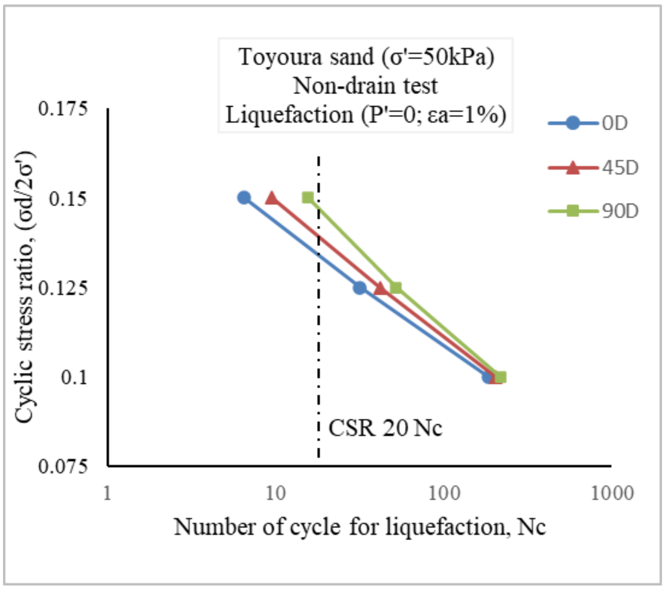

Fig. 10: Liquefaction resistance for 40% Relative density

liquefaction strength increased by increasing the particle angle. The 90° orientation case shows the maximum liquefaction strength compared to 0° and 45° because of their contact points of particles.

3.3 Re-liquefaction Resistance

Re-liquefaction test are conducted up to axial strain (ε_a) reaches 5% After the first liquefaction event, Toyoura sand tends to regain some strength through re-consolidation. From Fig. 11, re-liquefaction strength shows the opposite scenario compared to liquefaction at 90° particle orientation. At 0° and 45° the strength increased as usual as liquefaction, but strength decreased at 90°. This tendency can happen due to movement of soil particle moves towards 0°.

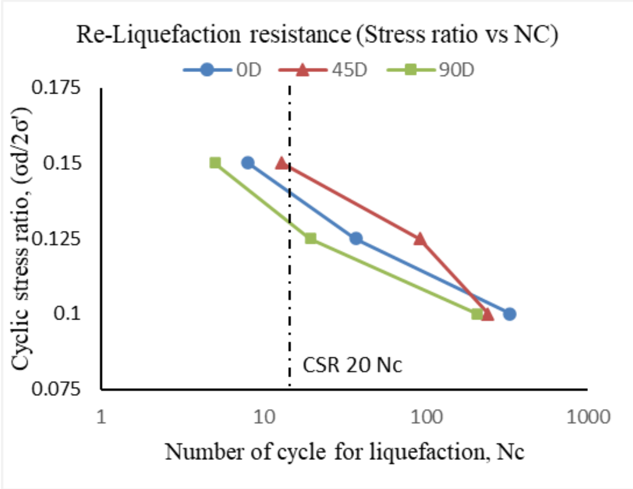

Fig. 11: Re-liquefaction resistance for 40% Relative density

At 0° particle orientation the average angle θ found 6.8° and vector magnitude was 45.9 that decreased (Fig. 12 a, b) to 27.2 after liquefaction. The tendency of soil particles is moved vertically and found the average angle 55.7 degree after liquefaction. That is the indication of strength increases in re liquefaction.

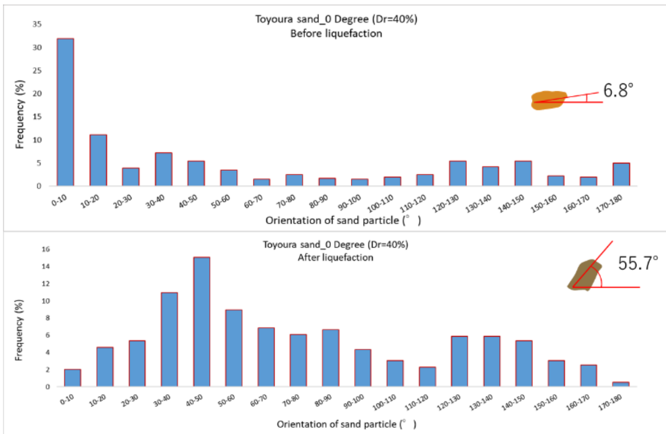

Fig. 12(a): Particle distribution of 0° before and after liq.

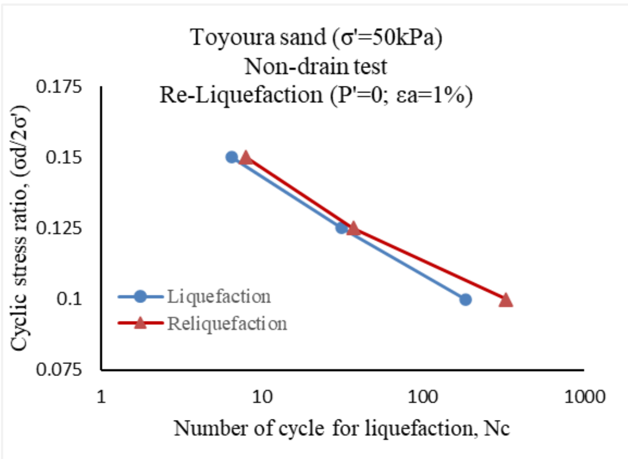

Fig. 12(b): liquefaction strength of 0° before and after liq.

The soil particle at 45° shows the same tendency (Fig. 13(a),(b)) as 0°. Particles move into more vertical that means the average angle are increased compared to before liquefaction.

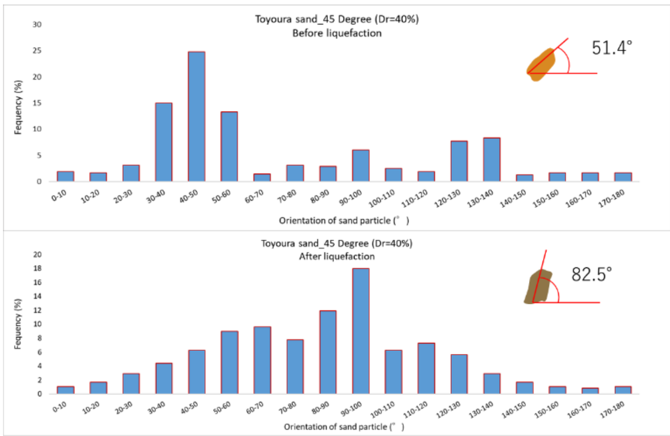

Fig. 13(a): Particle distribution of 45° before and after liq.

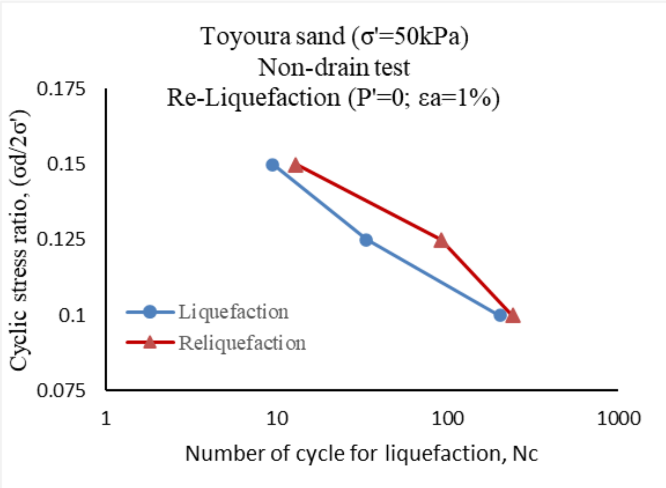

Fig. 13(b): liquefaction strength of 45° before and after liq.

In the case of 90° we see the opposite tendency (Fig. 14 a & b) of soil particle that moves horizontally. The average θ value and V.M both are decreased after liquefaction, that is the indication of lower strength during re-liquefaction.

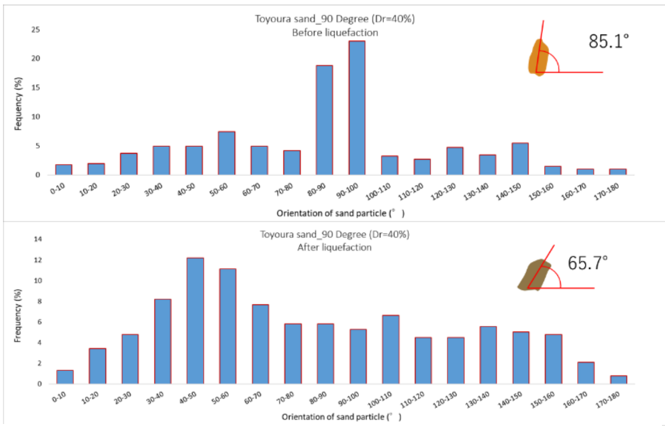

Fig. 14(a): Particle distribution of 90° before and after liq.

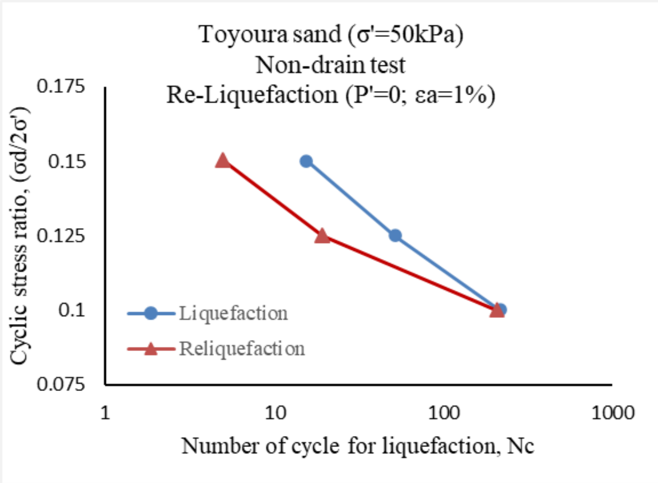

Fig. 14(b): liquefaction strength of 90° before and after liq.

Microscopic results show particle orientation after liquefaction of 0° and before liquefaction of 45° is almost the same, so the liquefaction resistance is also similar.

3.4 Effect of relative density

In this experiment, 40% relative density has been used. In most cases the relative density before liquefaction was around 40% and after liquefaction it increased a little around 2% to 3% that shown in table 2.

Table 2: Relative density before and after liquefaction

Particle orientation	q (Kpa)	Relative density (Dr) Before (%)	Relative density (Dr) After (%)	Increased Dr (%)
0°	10	44.78	47.33	2.55
45°		41.22	42.27	1.05
90°		38.42	41.73	3.31
0°	12.5	37.15	39.18	2.03
45°		39.44	41.73	2.29
90°		39.19	42.49	3.3
0°	15	39.95	41.48	1.53
45°		38.93	41.48	2.55
90°		39.19	42.24	3.05

4. Conclusion and Recommendations

4.1 Conclusion

- The study revealed that the liquefication strength (Nc) increased with particle orientation increases before liquefaction. The highest liquefaction strength was recorded at 90° before liquefaction but it decreased after liquefaction compared with 0° and 45°.

- The results indicated that relative density had no significant effect on the liquefaction strength, suggesting that the strength of the soil during liquefaction is not strongly influenced by the initial relative density.
- The shear modulus showed some variation, with larger values observed at 90° and 45° orientations compared to 0°. This suggests that soil samples at these orientations exhibit greater stiffness and resistance in very small strain range.
- The re-liquefaction strength demonstrated an increasing tendency for the 0° and 45° orientations, while a decrease was observed for the 90° orientation. This indicates that soil particles at 0° and 45° orientations become more stable upon repeated seismic events, whereas those at 90° show a reduction in alignment and strength.
- Microscopic examination showed that soil particles tend to move towards the 90° orientation during liquefaction. Conversely, particles at the 90° orientation exhibited a decrease in concentration (V.M) and moved towards 0°.

4.2 Recommendations

- Techniques such as densification and stabilization should be optimized based on the specific depositional structures of the soil to enhance liquefaction resistance effectively.
- Engineers should incorporate findings related to particle orientation and liquefaction resistance into the design of foundations to improve the resilience of structures in earthquake-prone areas.
- In this study, particle orientation was assessed using 2-D optical measurement. To gain a more comprehensive understanding, future research should employ 3-D measurement techniques to accurately capture the three-dimensional particle orientation.

References

1. Youd, T. L. (1973). Factors controlling maximum and minimum densities of sands. ASTM Special Technical Publication, (523), 98-112.

2. Seed, H. B., & Idriss, I. M. (1982). Ground motions and soil liquefaction during earthquakes (Vol. 5). Earthquake Engineering Research Institute.

3. Joseph R. Curray (1956). The Analysis of Two-Dimensional Orientation Data. The University of Chicago Press Journals, (Volume 64, Number 2).